

## The development of the seismic fragility curves of existing bridges in Indonesia (Case study: DKI Jakarta)

Veby Citra Simanjuntak<sup>\*1,2</sup>, Iswandi Imran<sup>1a</sup>,  
Muslinang Moestopo<sup>1b</sup> and Herlien D. Setio<sup>1c</sup>

<sup>1</sup>Structural Engineering Research Group, Faculty of Civil and Environmental Engineering,  
Bandung Institute of Technology, Indonesia, Ganesha 10, Bandung 40132, Indonesia

<sup>2</sup>Ministry of Public Works and Housing, Pattimura No. 20, Kebayoran Baru, Jakarta Selatan 12110, Indonesia

(Received February 14, 2023, Revised March 21, 2023, Accepted April 3, 2023)

**Abstract.** Seismic regulations have been updated from time to time to accommodate an increase in seismic hazards. Comparison of seismic fragility of the existing bridges in Indonesia from different historical periods since the era before 1990 will be the basis for seismic assessment of the bridge stock in Indonesia, most of which are located in earthquake-prone areas, especially those built many years ago with outdated regulations. In this study, seismic fragility curves were developed using incremental non-linear time history analysis and more holistically according to the actual strength of concrete and steel material in Indonesia to determine the uncertainty factor of structural capacity,  $\beta_c$ . From the research that has been carried out, based on the current seismic load in SNI 2833:2016/Seismic Map 2017 (7% probability of exceedance in 75 years), the performance level of the bridge in the era before SNI 2833:2016 was Operational-Life Safety whereas the performance level of the bridge designed with SNI 2833:2016 was Elastic – Operational. The potential for more severe damage occurs in greater earthquake intensity. Collapse condition occurs at  $A_s = F_{PGA} \times PGA$  value of bridge Era I = 0.93 g; Era II = 1.03 g; Era III = 1.22 g; Era IV = 1.54 g. Furthermore, the fragility analysis was also developed with geometric variations in the same bridge class to see the effect of these variations on the fragility, which is the basis for making bridge risk maps in Indonesia.

**Keywords:** fragility curve; performance level; seismic detailing; seismic loading codes; seismic vulnerability

### 1. Introduction

Indonesia is an earthquake-prone country and the earthquakes have caused the collapse and damage to several infrastructures including bridges. Seismic regulations from time to time have been updated to accommodate the increasing hazard along with the occurrence of damaging earthquakes in Indonesia (the Aceh earthquake accompanied by the tsunami in 2004 (Mw = 9.2), the Nias earthquake in 2005 (Mw = 8.7), the Jogja earthquake in 2006 (Mw = 6.3), Padang earthquake in 2009 (Mw = 7.6), Palu earthquake accompanied by the tsunami in 2018 (Mw = 7.4), Lombok

\*Corresponding author, Ms., E-mail: vebycitra.s@gmail.com

<sup>a</sup>Professor, E-mail: iswandiimran@gmail.com

<sup>b</sup>Ph.D., E-mail: mmoestopo@gmail.com

<sup>c</sup>Professor, E-mail: setioherlien@gmail.com

earthquake in 2018 ( $M_w = 6.4$ ). For example, for the DKI Jakarta area, the PGA value is set at 0.15 g on the Seismic Map 2002 (10% probability of exceedance in 50 years or Return Period (RP)= 500 years) and 0.25-0.30 g on Seismic Map 2010 and Seismic Map 2017 (7% probability of exceedance in 75 years (RP= 1000 years)).

Updating of seismic regulations certainly has implications for tighter provisions on bridge seismic detailing. These implications raise questions regarding the seismic performance of the existing bridges that were designed and built many years ago, but are still operating now. Therefore, there is a significant need to evaluate the existing bridges before future seismic events, especially those located in high seismic zones. Therefore, this research aimed to identify the seismic detailing from different versions of Indonesian bridge design codes before 1990 until now and to present the significant changes in the seismic performance level of the existing bridges built in different design eras through analytical fragility curves. Fragility curves show the magnitude of the probability value of a level of damage that occurs to the bridge due to various earthquake intensity levels. This is the basis for making bridge risk maps in Indonesia.

Several bridge fragility assessments with analytical fragility curves have been carried out so far in several countries for different classes of bridges. Fragility curve methodologies using analytical approaches have become widely adopted because they are more readily applied to bridge types and geographical regions where seismic bridge damage records are insufficient (Kibboua 2011). Researchers from various countries (Choi *et al.* 2004, Nielson and DesRoches 2007a, b), Ramanathan, *et al.* (2012), Billah and Alam (2015) in America, Mitchell, *et.al.* (2010) in Canada, Simon and Vigh (2016) in Hungary, Moschonas *et al.* (2009) in Greece, Karim and Yamazaki (2007) in Japan, Av ar Ö. (2012) in Turkey, Beilic *et al.* (2017) in Italy, Waseem (2017) in Pakistan, and Shekhar *et al.* (2019) in India, have developed analytical fragility curves for bridges in certain areas. Since seismic hazard, construction practice, design code, seismicity and soil conditions are different for each region, the existing studies focus on developing the fragility curve per region, as also stated in the study by Simon and Vigh (2017). Thus, it is necessary to analyze the seismic fragility of existing bridge structures in Indonesia against seismic conditions based on an updated earthquake hazard map. Evaluation is required to see the potential for structural damage that may happen if a specific earthquake scenario occurs. It will also serve as the basis for retrofitting to maintain performance.

In this study, the analysis of the fragility of existing bridges in Indonesia was also developed more holistically according to the actual material data in Indonesia to determine the uncertainty of the structural capacity,  $\beta_c$  in the formation of the fragility curve. The fragility analysis was also developed with geometric variations to see the effect of these variations on the fragility curve in the same bridge class. The bridge structure analyzed was located in the DKI Jakarta area as a strong earthquake zone in Indonesia. The focus of the research was a multi-span girder concrete bridge which was the bridge with the largest population and contributes more than 50% to the national bridge stock based on data from the Directorate General of Highways Ministry of Public Works and Housing, Indonesia (2021). It can be found in every era of bridge. However, this study focused on the influence affected by the level of strictness of Indonesian seismic design codes for the bridge.

## 2. Seismic design provisions in Indonesia

Fig. 1 shows the development of bridge design regulations and earthquake maps in Indonesia and the most recent bridge design requirements are SNI 2833:2016 and Seismic Map 2017 (1000 year

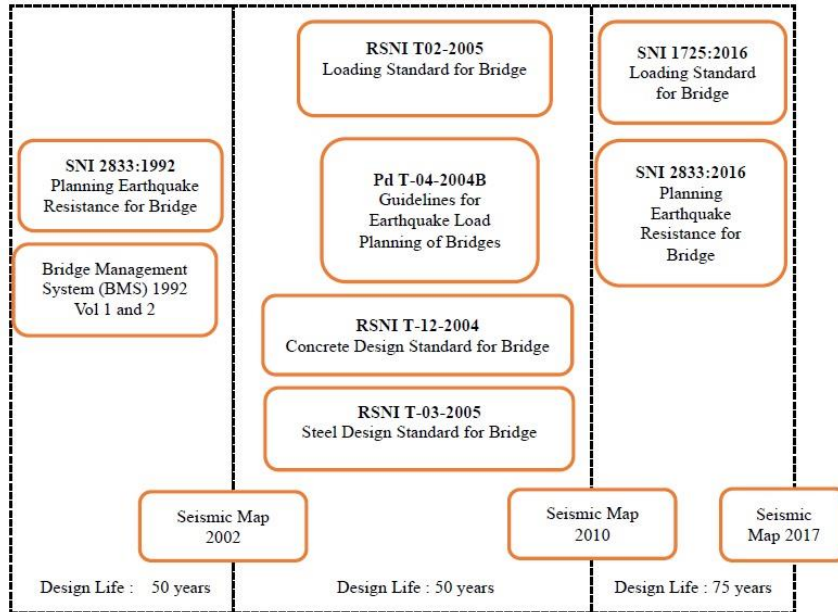


Fig. 1 Development of bridge regulations in Indonesia

Table 1 Indonesian seismic codes differences

Aspects	PBI 1971/PMI 1970	BMS 1992	Pd T-04-2004-B	SNI 2833:2008	SNI 2833:2016
Location	$L = \max \begin{cases} \text{column } \varnothing \\ \frac{1}{6}H \\ 450 \text{ mm} \end{cases}$		$L = \max \begin{cases} 1.5 \text{ column } \varnothing \\ \frac{1}{4}H \\ 600 \text{ mm} \end{cases}$		$L = \max \begin{cases} \text{column } \varnothing \\ \frac{1}{6}H \\ 450 \text{ mm} \end{cases}$
Plastic hinge region detailing	$\begin{cases} \frac{1}{2} * 0.45 h s \left(\frac{A_g}{A_c} - 1\right) \frac{f_c'}{f_{yh}} \\ \frac{1}{2} * 0.12 \frac{f_c'}{f_{yh}} h s \end{cases}$	$\rho_s \geq \max \begin{cases} 0.45 \left(\frac{A_g}{A_c} - 1\right) \frac{f_c'}{f_{yh}} \\ 0.12 \frac{f_c'}{f_{yh}} \end{cases}$ Square stirrups may be used and the area of reinforcement in each major direction of the cross-section greater than: $A_{sh} = 0,3 s_h h_c$ $\left(\frac{A_g}{A_c} - 1\right) \frac{f_c'}{f_{yh}}$ or $A_{sh} = 0,12 s_h h_c \frac{f_c'}{f_{yh}}$	The volume of a closed spiral or circular is determined from the largest value of: $\rho_s \geq \max \begin{cases} 0.45 \left(\frac{A_g}{A_c} - 1\right) \frac{f_c'}{f_{yh}} \\ 0.12 \frac{f_c'}{f_{yh}} \end{cases}$ $\rho_s \leq 0.018$ Square stirrups may be used and the area of reinforcement is the greater of: $A_{sh} = 0,3 s_h h_c \left(\frac{A_g}{A_c} - 1\right) \frac{f_c'}{f_{yh}}$ or $A_{sh} = 0,12 s_h h_c \frac{f_c'}{f_{yh}}$	Shear strength $V_s \leq 0.67 \sqrt{f_c'} A_e$ with $A_e = 0,8 A_g$  The area of shear reinforcement for each column core restrained by spiral reinforcement or stirrups must be greater than the given value: $A_v \geq 0.17 \frac{D's}{f_{yh}}$	
	Confining steel	Min: 15 db; Smallest of section dimension; 100mm		$s \leq \min \begin{cases} 200 \text{ mm} \\ 6d_b \end{cases}$	
Longitudinal reinforcement	-	$0.008A_g \leq \rho \leq 0.06A_g$		$0.01A_g \leq \rho \leq 0.04A_g$	

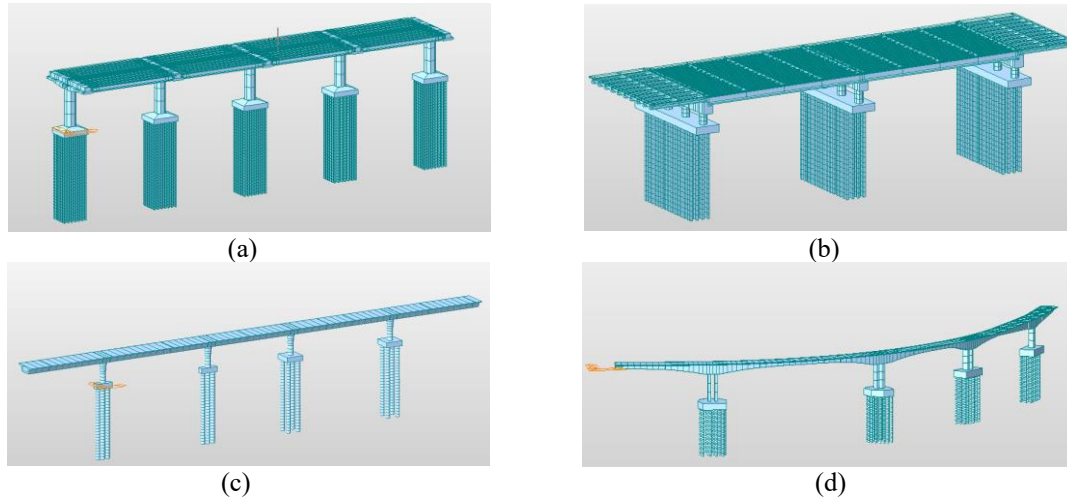


Fig. 2 Bridge modeling in Midas Civil 2019 (a) Cawang-Tanjung Priuk Bridge (Era I), (b) Pesanggrahan Bridge (Era II), (c) Antasari-Blok M Bridge (Era III) and (d) Becakayu Bridge (Era IV)

earthquake hazard level with 7% probability of exceedance in 75 years). Table 1 provides a comparison of seismic detailing provisions in various Indonesian bridge codes. The history of fundamental changes to these regulations in more detail, especially related to seismic provisions, is stated in another study by Simanjuntak *et al.* (2022).

### 3. Methods

To illustrate the changes in seismic performance of existing bridges in each era, which of course, also determines the design code used, multi-span reinforced concrete girder in Jakarta as the bridge with the largest population (>50%) in the DKI Jakarta was chosen. In Era I and II, simply-supported bridges were the most frequent class in the stock. Meanwhile, in Era III and IV, multi-span continuous bridge and monolithically connected to the deck were quite a lot to find in the bridge stock. As-built drawings were collected from the various departments of transportation and examined to determine pier details as Earthquake Resisting Elements (ERE).

#### 3.1 Bridge characteristics

Brief descriptions of the four bridge that are used in this study are provided below and modeling in Midas Civil 2019 can be seen in Fig. 2.

- Era I - Before the 1990s

The bridge structure studied was Cawang-Tanjung Priuk Bridge (STA 20+641,549 – STA 20+676,549) (P.188) which was located on Wiyoto Wiyono Toll Road in North Jakarta (Jakarta Inner Ring Road- JIRR). The bridge was built before 1990, referring to the PMI 1970 earthquake regulation. The bridge is simply supported by a single pier. Based on data obtained, the technical data of the structure: (a) span length: 35 m (b) number of girder: 10 girders (c) wide span bridge: 25 m (d) pier height: 13,2 m (e) diameter of pier: 3,5 m (f)  $f_c'$ : 29,05 MPa;  $f_y$ : 400 MPa (g) tendon prestress PC-7-Wire, ASTM A-416, Grade 270. The detailing and

configuration of pier reinforcement: (a) longitudinal rebar: 144 D32 (b) transverse rebar ratio: 0,005 (c) transverse rebar spacing: 100 mm.

- Era II - BMS 1992

The bridge structure studied was Pesanggrahan Bridge which was located on (Jakarta Outer Ring Road-JORR W-2), referring to the BMS 1992. The construction of the bridge was completed in 2003. Based on data obtained, the technical data of the structure: (a) span length : 13,482 m – 35,03 m -35,03 m – 13,53 m (b) number of girder : 10 girders (c) wide span bridge : 24,25 m (d) pier height : 4,469 m (e) diameter of pier: 1,5 m (f)  $f_c'$  : 29,05 MPa;  $f_y$  : 400 MPa (g) tendon prestress PC-7-Wire, ASTM A-416, Grade 270. The detailing and configuration of pier reinforcement: (a) longitudinal rebar: 48D32 (b) transverse rebar ratio: 0,015 (c) transverse rebar spacing: 150 mm.

- Era III - 2004-2016

The bridge structure studied was Non-Toll Flyover Antasari-Blok M which was located in South Jakarta, referring to the SNI 2833:2008. The construction of the bridge was completed in 2012. The bridge is Multi-span – Continuous Prestressed Concrete Box Girder. Based on data obtained, the technical data of the structure: (a) span length : 35-40 m (b) wide span bridge : 9 m (c) pier height : 7,6 m (d) diameter of pier: 2,0 m (e)  $f_c'$  : 29,05 MPa;  $f_y$  : 400 MPa (f) tendon prestress PC-7-Wire, ASTM A-416, Grade 270. The detailing and configuration of pier reinforcement: (a) longitudinal rebar: 90 D32 (b) transverse rebar ratio: 0,009 (c) transverse rebar spacing: 100 mm.

- Era IV – Post-2016

The bridge structure studied was Becakayu NS Link, referring to the SNI 2833:2016. The construction of the bridge was completed in 2018. The bridge is Multi-span – Continuous Prestressed Concrete Box Girder (Balanced Cantilever). Based on data obtained, the technical data of the structure: (a) span length : 93,618 m -103,35 m- 97,25 m -55,41 m (b) wide span bridge : 14 m (c) pier height : 16,6 m (d) dimension of pier: 5,0 m x 2,0 m (e)  $f_c'$  : 41,5 MPa;  $f_y$  : 400 MPa (f) tendon prestress PC-7-Wire, ASTM A-416, Grade 270. The detailing and configuration of pier reinforcement: (a) longitudinal rebar: 280 D32 (b) transverse rebar ratio:  $p_x = 0,025$ ;  $p_y = 0,007$  (c) transverse rebar spacing: 100 mm.

### 3.2 Inelastic modeling

For inelastic modeling, the cross-sectional moment-curvature relationship must first be calculated in order to derive the rotational moment connection. The rotation value was then determined by multiplying the curvature value by the length of the plastic hinge. The moment-curvature of sections was generated from XTRACT (TRC 2010). The inelastic behavior using the Mander Model (Mander *et al.* 1988) to describe the inelastic behavior of the concrete material and the Bilinear with Strain Hardening model to describe the stress-strain relationship in the steel material (Fig. 3).

Nonetheless, monotonic analysis overestimates strength capacity. The cyclic condition will more accurately describe inelastic seismic demands. Continuous monotonic loads will result in a significant drop in strength and energy, hence the effect of cyclic loads, such as earthquakes, must be considered. Modifying the monotonic backbone curve parameters of the XTRACT output ( $\theta_p^* = 0.7 \theta_p$ ;  $\theta_{pc}^* = 0.5 \theta_{pc}$ ) as given by PEER/ATC72-1 can be used to define the parameters of the first cycle envelope model. The inelastic hysteresis behavior of the pier in Midas Civil 2019 was defined by a skeleton curve and applied to the pier's flexural component, namely the bending

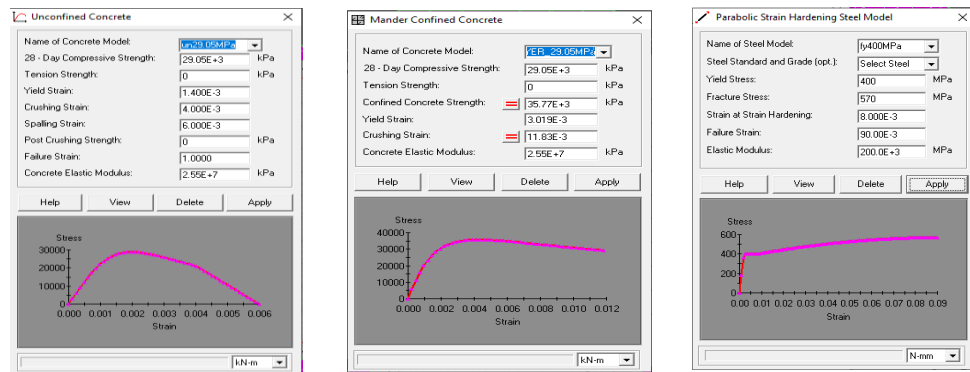


Fig. 3 Material properties pier section on XTRACT

moment around the local y-axis ( $M_y$ ) to the local z-axis ( $M_z$ ), which was specified by the rotational moment relationship of each pier element. The Takeda Hysteresis model, which simulates the inelastic behavior of concrete under cyclic loads, was used in this study.

### 3.3 Selection of ground motion and non-linear time history analysis (NLTHA)

An analysis of the response of the bridge was carried out using incremental NLTHA with 7 (seven) sets of ground motion as required in AASHTO LRFD Bridge Design Specifications 2011. The appropriate ground motions are selected from the recording of actual earthquake events which have magnitude ( $M$ ), fault distance (mean-source distance  $R$ ) and earthquake source mechanism through a deaggregation process. Table 2 below shows the specific seismic characteristics of the Jakarta site that have been selected and developed by Hutapea *et al.* (2015) through the Probabilistic Seismic Hazard Analysis (PSHA) and also stated in Indonesia Seismic Hazard Deaggregation Map for Earthquake Resistant Infrastructure Planning and Evaluation by the National Center for Earthquake Study (2022). Furthermore, the amplitude scaling process was carried out to produce ground motion input compatible with the Target Response Spectrum so that it was not less than the spectra acceleration of the Target Response Spectrum in the period range of 0.5 T to 2.0 T as referred to in the AASHTO Guide Specifications for LRFD Seismic Bridge Design 2011. Each ground motion produces a different scale factor and the scale factor was applied to the time history in Midas Civil 2019.

The earthquake force was increased gradually from 0.1g to 2.0g with an increase every 0.1g, so that the distribution of maximum displacement values was obtained for Slight Damage, Moderate Damage, Extensive Damage and Complete Damage conditions (Vamvatsikos 2002). The illustrations of the damage level that experienced varying seismic intensity were then be processed

Table 2 Deaggregation and ground motion characteristics of Jakarta for the 1000-year return period

No	Source	M	R (km)
1	Megathrust	8.7	171
2	Shallow Crustal	5.9	51
3	Benioff	6.9	122

to develop a fragility curve. Meanwhile, for short bridges, the influence of seismic spatial ground motion variability causes a relatively small increase in the peak response value so relatively unimportant in comparison to effects of differential site response (seismic traveling wave effect) (AASHTO LRFD Bridge Design Specifications - Section 3.4.4 (2011), Shinozuka *et al.* (2000, 2007), Han *et al.* (2015))

### 3.4 Damage states and performance level

One of the most important and challenging steps in seismic vulnerability is the determination of the corresponding limit states. In this study, the seismic response of the pier as Earthquake Resisting Elements (ERE) was analyzed. Both longitudinal and transversal response was checked. By taking the maximum average value of the drift value as the Engineering Demand Parameter (EDP) on the pier element due to 7 (seven) earthquake pairs, the performance levels could be determined and implemented following NCHRP 440's Acceptance Criteria (Table 3) by calculating the drift from the steel strain and concrete strain limits where  $\phi = \frac{\epsilon_c}{kd} = \frac{\epsilon_s}{d(1-k)} = \frac{\epsilon_c + \epsilon_s}{d}$  and  $\theta = \phi \times L_p$  and drift =  $\theta \times h_{pier}$ . Based on HAZUS-MH (FEMA 2003), the identification of the structure's earthquake damage level was also qualitatively described (Table 4). Meanwhile, for performance-based evaluation, this study adopted the 2020 version of the NCHRP 949 Guidelines as also referred to in the study by Lim *et al.* (2021). Table 5 shows that with a hazard 1000-year seismic load, the

Table 3 Bridge performance level (NCHRP 440, 2013)

Level	Description	Steel Strain	Concrete Strain	% Drift	Displacement Ductility
II	Operational	<0,005	<0,0032	<1	<1
III	Life Safety	0,019	0,01	3	2
IV	Near Collapse	0,048	0,027	5	6
V	Collapse	0,063	0,036	8,7	6

Table 4 Description of bridge damage levels based on HAZUS

Damage Level	Description
Slight/Minor Damage	Minor cracking and spalling to the abutment, cracks in shear keys at abutments, minor spalling and cracks at hinges, minor spalling at the column (damage requires no more than cosmetic repair) or minor cracking to the deck
Moderate Damage	Any column experiencing moderate (shear cracks) cracking and spalling (column structurally still sound), moderate movement of the abutment (<2”), extensive cracking and spalling of shear keys, any connection having cracked shear keys or bent bolts, keeper bar failure without unseating, rocker bearing failure or moderate settlement of the approach
Extensive Damage	Any column degrading without collapse – shear failure - (column structurally unsafe), significant residual movement at connections, or major settlement approach, the vertical offset of the abutment, differential settlement at connections, shear key failure at abutments.
Complete Damage	Any column collapsing and connection losing all bearing support, which may lead to imminent deck collapse and tilting of substructure due to foundation failure.

Table 5 Performance-based evaluation (NCHRP 949 Guidelines)

Earthquake Ground Motion	Bridge Importance and Service Life Category					
	Standard			Essential		
	ASL 1	ASL 2	ASL 3	ASL 1	ASL 2	ASL 3
<b>Lower-Level Ground Motion</b> 50% probability of exceedance in 75 years; the return period is about 100 years	PL0	PL3	PL3	PL0	PL3	PL3
<b>Upper-Level Ground Motion</b> 7% probability of exceedance in 75 years; return period is about 1000 years	PL0	PL1	PL1	PL0	PL1	PL2

**Notes:**

Anticipated Service Life categories are ASL 1 : 0-15 years; ASL 2 : 16-50 years; ASL 3 : &gt; 50 years

Performance Levels are:

**PL0:** No minimum level of performance is recommended**PL1:** Life Safety, Significant damage is sustained and service is significantly disrupted, but life safety is preserved. The bridge may need to be replaced after a large earthquake.**PL2:** Operational, Damage sustained is minimal and service for emergency vehicles should be available after inspection and clearance of debris. The bridge should be repairable with or without restrictions on traffic flow.**PL3:** Fully Operational, No damage is sustained and full service is available for all vehicles immediately after the earthquake. No repairs are required.

performance requirement is “**Life Safety**”. This is in line with AASHTO LRFD Bridge Design Specifications - Section 3.2 (2011) that bridges shall be designed for “Life Safety” performance objective considering a seismic hazard corresponding to a 7% probability of exceedance in 75 year. The bridge was allowed to suffer damage but not collapse.

### 3.5 Assessment of bridge fragility due to earthquake

Fragility curve that provides a relationship between the probability value of the occurrence of a level of damage (Damage State / DS) in the structure and the value of the earthquake intensity (Intensity Measure / IM.) HAZUS models the probability value of the occurrence of a level of damage due to an earthquake intensity level as a cumulative value of the lognormal distribution which can be calculated using the following Eq. (1)

$$P[\text{Exceedence si}|\text{IM}] = \Phi\left[\frac{1}{\beta_{tot}} \ln \frac{\text{IM}}{\text{LSi}}\right] \quad (1)$$

where IM is intensity measure of the earthquake; Lsi is the median value of IM to reach a level of damage;  $\beta_{tot}$  is the uncertainty factor;  $\Phi$  is Standard Normal Cumulative Distribution Function. The three main factors of uncertainty are the uncertainty definition of the level of damage,  $\beta_{ds}$  (Slight, Moderate, Extensive and Complete), the uncertainty of structural capacity,  $\beta_c$  and the uncertainty of earthquake demand,  $\beta_d$ . The total variability is modeled by a combination of these three factors, assuming that they are independent stochastic and lognormal as stated in Eq. (2)

$$\beta_{tot} = \sqrt{\beta_{DS}^2 + \beta_C^2 + \beta_D^2} \quad (2)$$

From the above equation, the greater  $\beta$ , the greater the probability of achieving or exceeding a level of damage. In this study,  $\beta_{ds} = 0.4$ ,  $\beta_d = 0.45$  according to HAZUS (FEMA 2003). Meanwhile,  $\beta_c$  was quantified from the analysis of the actual variability of concrete and steel materials in Indonesia. Furthermore, selection of an appropriate IM is an important step in developing fragility relationship. The selection of an intensity measure for the assessment of seismic risk requires careful consideration that the IM has in predicting the extent of damage arising from seismic motion and an it is judged according to efficiency, practicality, proficiency, and sufficiency (Syner 2011, Kehila *et al.* 2021). For the case of the development of the bridge structure fragility curve in this study, the earthquake intensity measure was used according to the amplified spectra acceleration (Peak Surface Acceleration),  $A_s = F_{PGA} \times PGA$  considering DKI Jakarta was on soft ground, so that the earthquake input used was more precise using the intensity of the earthquake on the surface.

## 4. Results and discussion

### 4.1 Evaluation of seismic detailing condition

Referring to the detailing requirements of the most recent code SNI 2833:2016 (Table 1), the pier condition as an Earthquake Resisting Element for the bridge was checked. For bridge era I (prior to 1990), the minimum spacing requirements of transverse reinforcement in the plastic hinge region, plastic hinge length, and longitudinal reinforcement were met as required in SNI 2833:2016, however the confinement reinforcement ratio was still less than the minimum required ( $\rho_s < \rho_{s \text{ min}}$ ). Furthermore, in Era II (BMS 1992), the minimum spacing requirement of transverse reinforcement in the plastic hinge area was less strict than it is required in SNI 2833:2016 (min 1/4D or 100 mm), so in this study, that was categorized into partially confined. Fig. 4 illustrates the moment-rotation calculation for pier conditions in each design era using the as-built drawing's pier detailing parameters. The cross-section of the pier in Era IV, which is a totally confined pier, gives more ductility. Meanwhile, ductility is needed for the performance of earthquake-resistant structures because it is the key to ensure large deformations without collapsing. The same findings are also shown in other countries even in moderate seismic regions were given by Choi *et al.* (2004), Mithcell *et al.* (2010), Ramanathan *et al.* (2012), Simon and Vigh (2016), Crespi *et al.* (2020). Ignorance or underestimation of the seismic action and inadequate confinement reinforcement in a column are the main issues in pre-and post-seismic design considerations.

### 4.2 Nonlinear time history analysis and performance level

Performance levels can be determined by taking the maximum average value of the drift value as EDP on the pier element due to 7 (seven) earthquake pairs. Meanwhile, by comparing the drift from NLTHA results with the drift calculated from the steel and concrete strain limits on the Acceptance Criteria at NCHRP 440 (Table 6), the determination of the performance level was carried out, as seen in Table 7. From the results, due to the earthquake load on Seismic Map 2017 for Jakarta ( $A_s = F_{PGA} \times PGA = 0.4 \text{ g}$ ), the performance level of the bridge in the era before SNI 2833:2016/Seismic Map 2017 was Operational-Life Safety (LS) and the structure was identified as having moderate damage. Meanwhile, the performance level of the bridge designed with SNI 2833:2016 was Elastic – Operational. Furthermore, referring to the latest NCHRP 949 -

Performance-Based Evaluation (Table 5), it can be seen that with a hazard 1000-year seismic load, the performance requirement is “**Life Safety**”. Results show that the performance level of the bridge still satisfies the requirement of NCHRP 949, which is Life Safety under upper-level earthquake (return period 1000 years). Therefore, the existing bridge in Jakarta shows adequate capacity under the current seismic load SNI 2833:2016/Seismic Map 2017 (7% probability of exceedance in 75 years (RP= 1000 years)).

Table 6 Acceptance criteria based on drift limit of pie

Level	Description	Steel Strain	Concrete Strain	Drift			
				Bridge I	Bridge II	Bridge III	Bridge IV
II	Operational	<0,005	<0,0032	0,0833	0,0293	0,0508	0,0894
III	Life Safety	0,019	0,01	0,2605	0,0915	0,1587	0,2795
IV	Near Collapse	0,048	0,027	0,7000	0,2469	0,4284	0,7547
V	Collapse	0,063	0,036	0,9377	0,3292	0,5713	1,0062

Table 7 Performance level of the existing bridge in various eras

Bridge	Average Drift (m)	% Drift	Damage State	Performance Level
Era I (Before the 1990s)	0,1658	1,3%	Moderate Damage	Operational-Life Safety
Era II (1990-2004)	0,0526	1,17 %	Moderate Damage	Operational-Life Safety
Era III (2004-2016)	0,1242	1,63 %	Moderate Damage	Operational-Life Safety
Era IV (post-2016)	0,0854	0.56 %	Slight Damage	Elastic-Operational

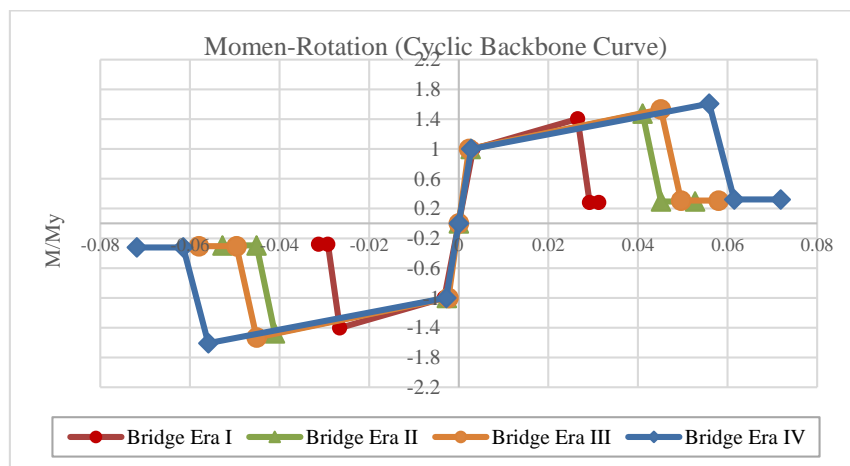


Fig. 4 Moment-rotation backbone curve for pier conditions in each design era

### 4.3 Material variability for uncertainty determination, $\beta_c$

In the seismic evaluation for the control deformation element, expected strength was used. In this study, the variability of the concrete quality  $f_c'$  and the quality of steel,  $f_y$  in Indonesia according to actual conditions in the field was analyzed, considering that the average value in the field was generally higher. Principally, referring to the FHWA, the expected strength can be taken by multiplying 1.2 for steel and 1.3 for concrete from the nominal strength or referring to Table B.3-1 AASHTO LRFD Bridge Design Specifications 9th Edition, 2020 which is  $1.25 f_y$  and  $1.5 f_c'$ . In this study, for the concrete material variability, the analysis was conducted from the test data for the compressive strength of concrete at the ready mix (5 plants/664 data) as shown in Fig. 5. Meanwhile, steel variability was obtained from the results of the tensile test results (984 data), as shown in Fig. 6. It can be concluded that the variation in steel quality was taken  $\pm 10\%$  as the standard deviation of the quality of reinforcing steel produced by Indonesian steel producers. This study assumed that

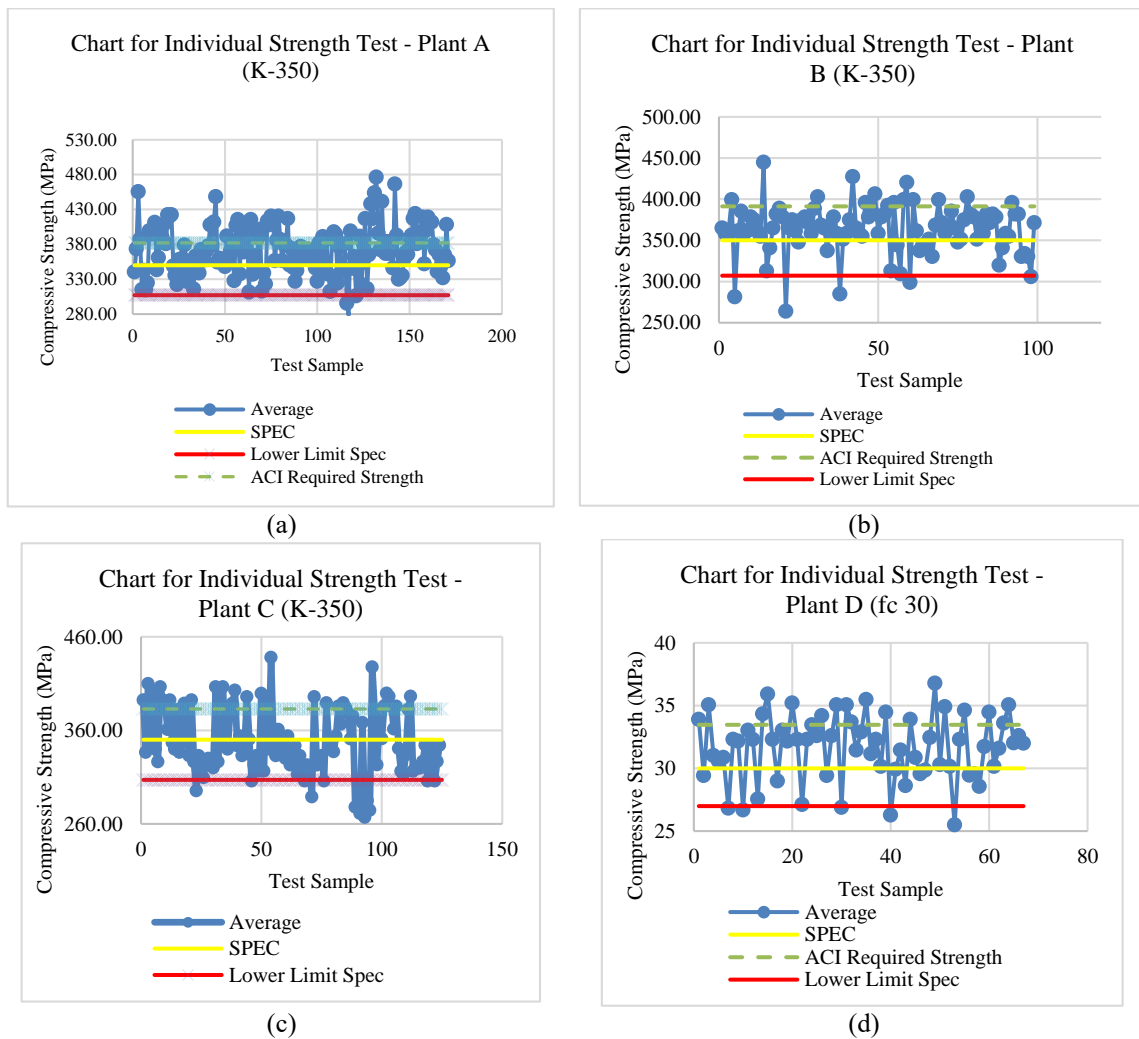


Fig. 5 Distribution of concrete compressive strength test results for  $f_c'$  30 (a) Plant A, (b) Plant B, (c) Plant C, (d) Plant D and (e) Plant E

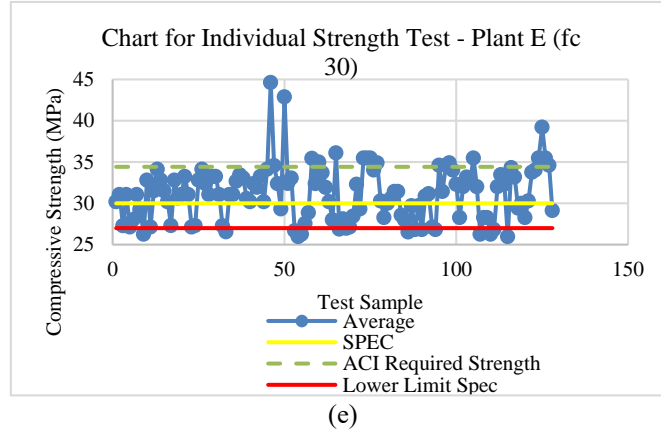


Fig. 5 Continued-

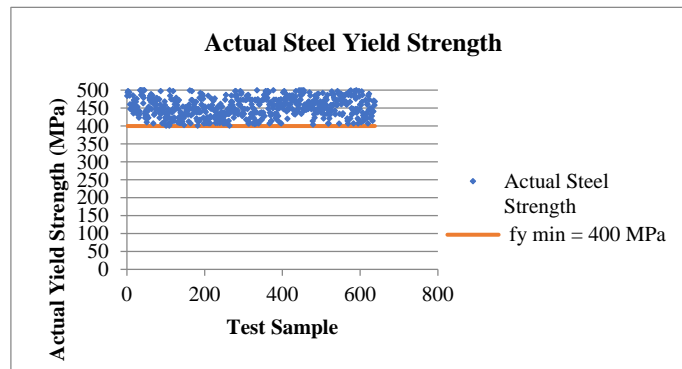


Fig. 6 Distribution of steel strength test results

Table 8 Actual variability of concrete and steel materials in Indonesia and structural capacity dispersion

Model	Expected Strength Ratio	fc' (MPa)	fy (MPa)	My (kN.m)	Mu (kN.m)	$\phi_y$ (1/m)	$\phi_u$ (1/m)	$\beta$ tot			
								Slight	Mode-rate	Extensive	Complete
Model 1 – fc' (nominal)	1.00	29.05	400	67930	95350	0.000914	0.01175	0.776	0.654	0.627	0.60
Model 2 – fc' (average)	1.08	31.23	400	67930	96360	0.000914	0.01179	0.776	0.654	0.627	0.60
Model 3 – fc' (max)	1.22	35.33	400	69100	97970	0.000894	0.01181	0.776	0.654	0.635	0.60
Model 4 – fy' (nominal)	1.00	29.05	400	67930	95350	0.000914	0.01175	0.776	0.654	0.627	0.60
Model 5 – fy (average)	1.13	29.05	452	74380	104400	0.001007	0.01216	0.776	0.654	0.643	0.60
Model 6 – fy (max)	1.31	29.05	524	74380	115500	0.001007	0.01275	0.776	0.720	0.643	0.60

the variations in production and technology in each era were the same. For confidentiality of ready mix data, the authors decide to use alphabetical.

Several bridges were then modeled with the expected strength of concrete and steel materials in Indonesia (Table 8) for evaluating the structural capacity dispersion ( $\beta_C$ ). From the results,  $\beta_C$  values were found to vary from 0.3-0.4. Using Eq. (2) by taking the value of  $\beta_{ds} = 0.4$ ,  $\beta_d = 0.45$ ,  $\beta_{tot}$  was obtained, which was about **0,6-0,78**.

#### 4.4 Seismic fragility curves across different design eras

The earthquake force was then increased gradually to illustrate the level of damage that experiences varying seismic intensity as shown in Table 9. Using Eq. (1) with the parameter values of  $LS_i$  and  $\beta_{tot}$ , the probability value of each level of damage was calculated by following the lognormal probability distribution:  $P[\text{Slight}|S_a]$ ,  $P[\text{Moderate}|S_a]$ ,  $P[\text{Extensive}|S_a]$ ,  $P[\text{Complete}|S_a]$ . Based on the fragility curve (CDF) (Fig. 7), due to the earthquake load on Seismic Map 2017 for Jakarta ( $A_s = F_{PGA} \times PGA = 0.4 \text{ g}$ ), the probability of extensive damage and complete damage for the bridge in era I were 15.8% and 7.19%, respectively. In other words, the potential damage that occurs was only slight and moderate damage. From another perspective, if the 50% probability level is taken by drawing a horizontal line cutting off the fragility curve then vertical line from the intersection to the  $A_s = F_{PGA} \times PGA$ , it can be concluded that for the bridge in era I, the  $A_s = F_{PGA} \times PGA$  values for the probability of exceeding >50% for each damage are 0.20 g for slight damage, 0.42 g for moderate damage; 0.73 g for extensive damage; 0.93 g for complete respectively. The recap for the probability of exceeding >50% for each damage in other eras can be seen in Table 10 and Figs. 7 and 8. This paper has clearly shown that the new Indonesian seismic bridge regulation had a major impact on the reduction of vulnerabilities of the bridge.

Table 9 Target response spectrum scenario and identification of performance level- Era I

$A_s = F_{PGA} \times PGA$ (g)	PGA (g)	Average ALL EQ (di)(meter)	Drift (%)	Damage State	Performance Level
0.10	0.07	0.0485	0.37	Slight Damage	<Operational
0.20	0.15	0.0955	0.72	Moderate Damage	Operational-LS
0.30	0.22	0.1427	1.08	Moderate Damage	Operational-LS
<b>0.40</b>	<b>0.27</b>	<b>0.1658</b>	<b>1.18</b>	<b>Moderate Damage</b>	<b>Operational-LS</b>
0.50	0.37	0.2056	1.56	Extensive Damage	LS-Near Collapse
0.60	0.45	0.2316	1.75	Extensive Damage	LS-Near Collapse
0.70	0.52	0.2701	2.05	Extensive Damage	LS-Near Collapse
0.80	0.60	0.3253	2.46	Extensive Damage	LS-Near Collapse
0.90	0.67	0.3684	2.79	Extensive Damage	LS-Near Collapse
1.00	0.75	0.4172	3.16	Complete Damage	NC-Collapse
1.10	0.82	0.4461	3.38	Complete Damage	NC-Collapse
1.20	0.90	0.4788	3.63	Complete Damage	NC-Collapse
1.30	0.97	0.5205	3.94	Complete Damage	NC-Collapse
1.40	1.05	0.5557	4.21	Complete Damage	NC-Collapse
1.50	1.12	0.5924	4.49	Complete Damage	NC-Collapse

#### 4.5 Effect of geometric properties on bridge fragility

Furthermore, the effect of bridge geometry on seismic fragility was evaluated by integrating the fragility function on the governing geometry parameters span length ( $L_{span}$ ) and column height ( $h_{pier}$ ) with a logistic regression analysis approach. With this simplification approach, it is possible to estimate the probability level of damage to several bridges in the same class (Karim and Yamazaki 2003) for seismic assessment of a bridge stock. From the results, the pier height significantly affects the fragility curve, where a higher pier is more susceptible to seismicity as seen from the significant rate of change of IM. (Fig. 9). For the probability of exceeding  $>50\%$  (collapse), a twofold increase in  $h_{pier}$  gives an IM difference of 0.3-0.4 g. Meanwhile, the seismic fragility for span length variations in the simply-supported bridge class (Era I&II) looks insensitive but in the continuous bridge class (Era III & IV), it can be seen that the longer the span, the greater the fragility. This is because, in continuous bridges, the span length plays a vital role in the distribution of internal forces

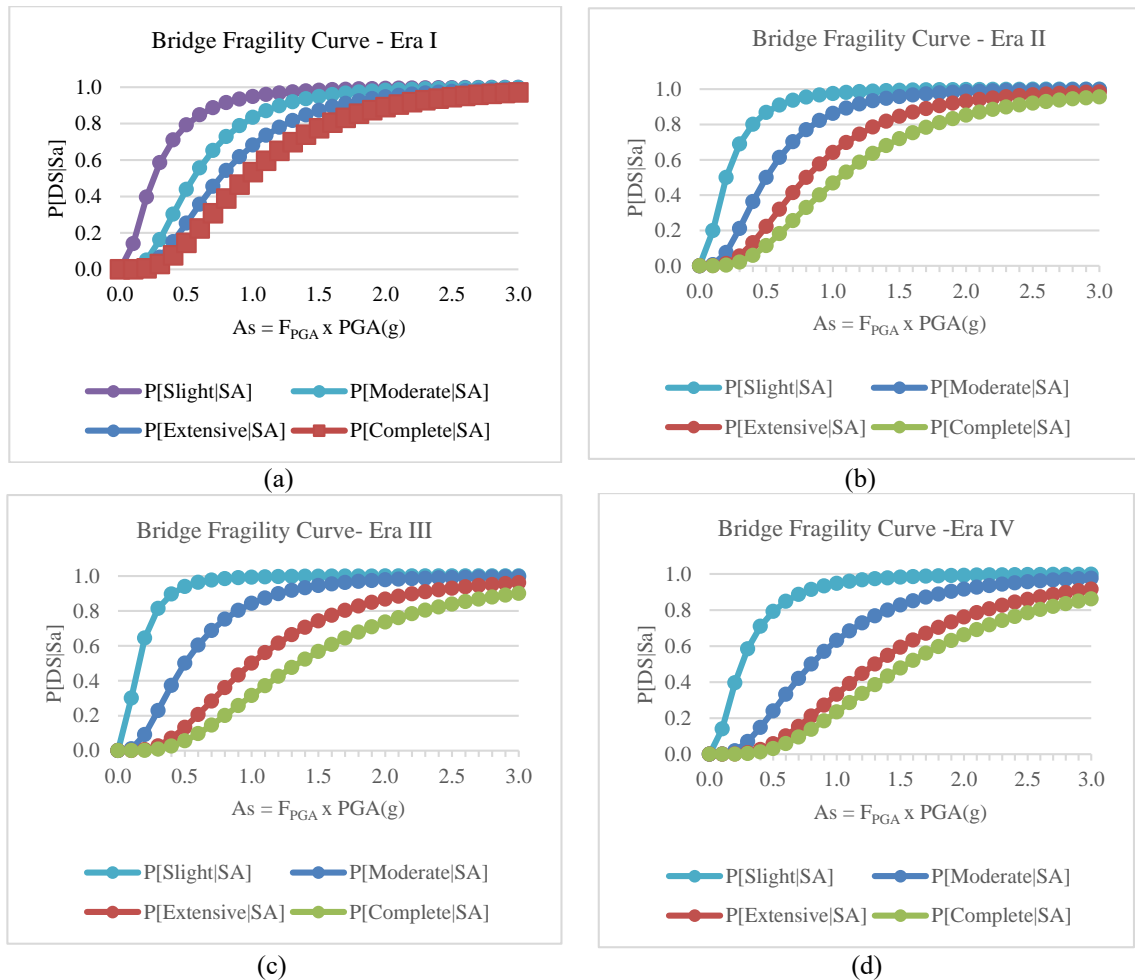


Fig. 7 Seismic fragility curves across different design eras (a) Era I, (b) Era II, (c) Era III and (d) Era IV

Table 10 Recap of  $A_s = F_{PGA} \times PGA$  for each damage condition for the probability of exceeding >50%

	Era I	Era II	Era III	Era IV
Slight	0.20 g	0.25 g	0.35 g	0.40 g
Moderate	0.42 g	0.44 g	0.45 g	0.8 g
Extensive	0.73 g	0.8 g	0.9 g	1.3 g
Complete	0.93 g	1.03 g	1.22 g	1.54 g

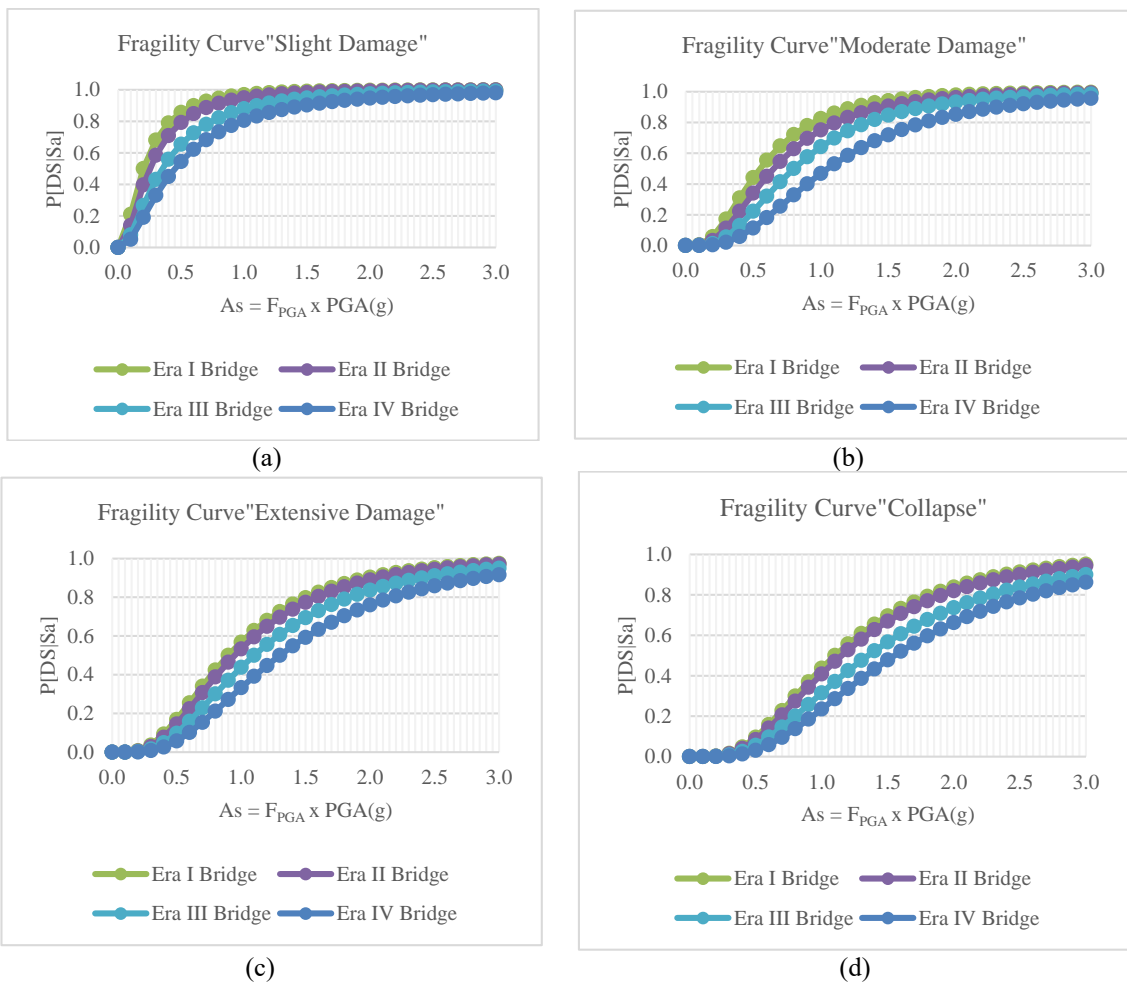


Fig. 8 Bridge fragility curves for each damage level (a) Slight Damage, (b) Moderate Damage, (c) Extensive Damage and (d) Collapse

(stiffness distribution) as shown in Fig. 10. The sensitivity study revealed that the volumetric ratio of transverse reinforcement, substructure type, span length and column height were the most significant ones affecting the seismic fragility, as also stated in the study by Olmos *et al.* (2012) and Dukes *et al.* (2018).

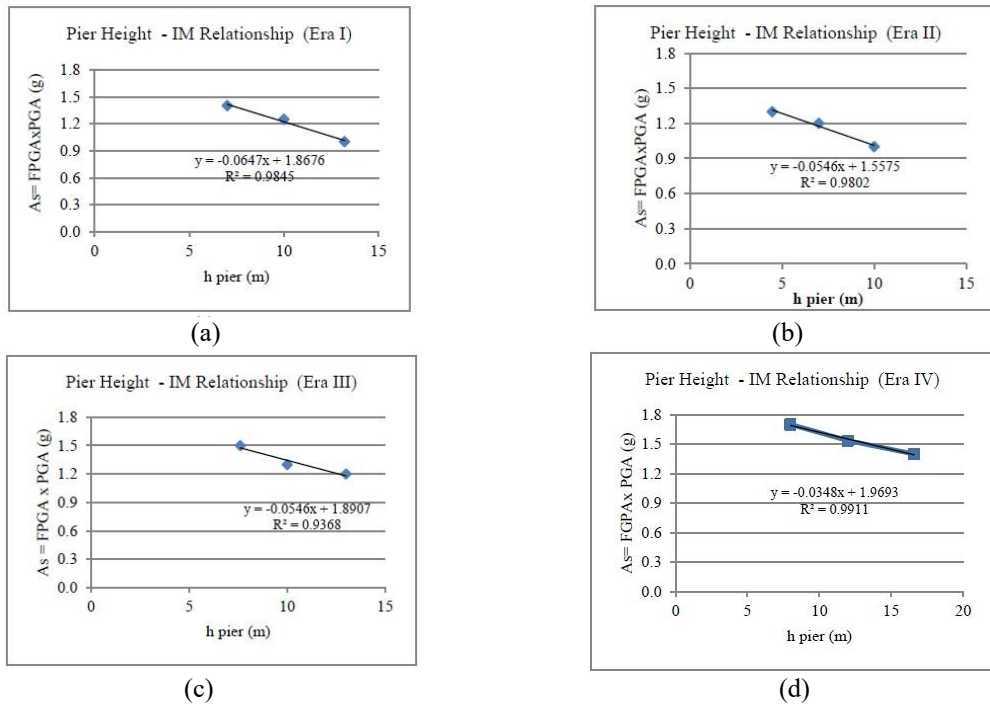


Fig. 9 Effect of pier height on seismic fragility in each era (a) Era I, (b) Era II, (c) Era III and (d) Era IV

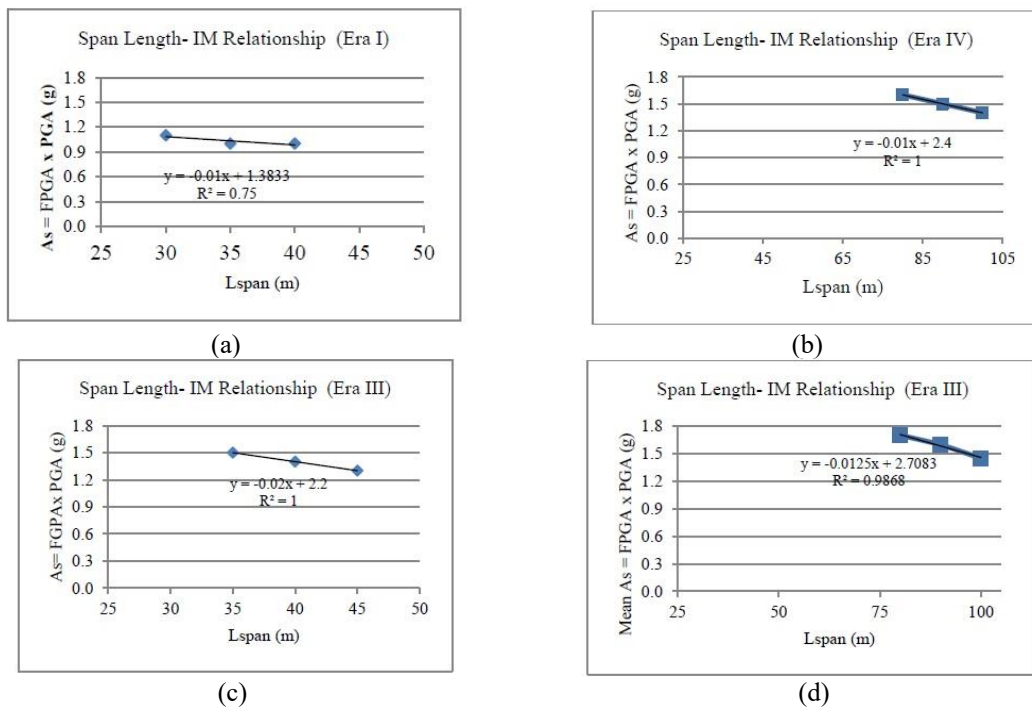


Fig. 10 Effect of span length on seismic fragility in each era (a) Era I, (b) Era II, (c) Era III and (d) Era IV

## 5. Conclusions

This paper provided a comprehensive summary of seismic fragility analysis of existing bridges from each era (before 1990 to the present). It was also developed more holistically according to the actual material data in Indonesia, which can be used as the basis for bridge evaluation in Indonesia. According to the sensitivity study, the volumetric ratio of transverse reinforcement, span length and column height were the most significant ones affecting the seismic fragility. It was found that in Indonesia's bridge code before SNI 2833:2016, inadequate confinement and limited ductility were the main issues. The performance of older bridges would typically be less than more recently designed structures. The performance level of the bridges in the eras before SNI 2833:2016/Seismic Map 2017 was Operational-Life Safety (LS) whereas the performance level of bridge designed with SNI 2833:2016 was Elastic – Operational. However, the performance level of the bridge still satisfies the requirement of NCHRP 949, which is "Life Safety" under upper-level earthquake (return period 1000 years). Therefore, the existing bridge shows adequate capacity under the current seismic load SNI 2833:2016/Seismic Map 2017 ((7% probability of exceedance in 75 years (RP= 1000 years)). The potential for more severe damage occurs in earthquakes with greater earthquake intensity. Collapse condition occurs at  $A_s = F_{PGA} \times PGA$  (g) value of bridge Era I = 0.93 g ; Era II = 1.03 g ; Era III = 1.22 g ; Era IV = 1.54 g. The results show that the fragility curve of the bridge in Era IV is gentler than the fragility curve in the previous era, indicating that it was less vulnerable. This paper has clearly shown that the evolution of seismic design codes had a major impact on the reduction of vulnerabilities of the bridge.

Furthermore, the pier height significantly affects the fragility curve, where a higher pier is more susceptible to seismicity as seen from the significant rate of change of IM. For the probability of exceeding >50% (collapse), a twofold increase in  $h_{pier}$  gives an IM difference of 0.3 g for the probability of exceeding >50% (collapse). Meanwhile, the seismic fragility for span length variations in the simply-supported bridge class looks insensitive but in the continuous bridge class, it can be seen that the longer the span, the greater the fragility. This is because in continuous bridges, span length plays an important role in the distribution of internal forces (stiffness distribution).

This study's findings can be used to estimate the probability level of damage to several bridges in the same class (type of pier, deck, pier to deck connection) for seismic assessment of a bridge stock, as the basis for making bridge risk maps in Indonesia. This research method is expected to be applied as framework in other areas in Indonesia. Considering that the results obtained in this study are for the geological conditions at the case study location and for the multi-span concrete girder bridge structure type only, so for the future work, it is fairly important to explore the observations for a more complete type of bridge in various regions in Indonesia. Another important aspects that deserves attention are deterioration such as aging (spalling of reinforced concrete, corrosion of the column reinforcement) and also the seismic traveling wave effect if the bridge under study is long-span bridge (non-standard bridge).

## References

- American Association of State Highway and Transportation Officials (2011), *Guide Specifications for LRFD Seismic Bridge Design*, In Subcommittee T-3 for Seismic Effects on Bridges, USA.
- American Association of State Highway and Transportation Officials (2020), *AASHTO LRFD Bridge Design Specification 9th Edition*, Washington, USA.

- ATC 72-1 (2010), *Modelling and Acceptance Criteria for Seismic Design and Analysis of Tall Buildings*, PEER/ATC
- Avsar, Ö. and Yakut, A. (2012), "Seismic vulnerability assessment criteria for RC ordinary highway bridges in Turkey", *Struct. Eng. Mech.*, **43**(1), 127-145. <https://doi.org/10.12989/sem.2012.43.1.127>.
- Beilic D. *et al.* (2017), "Seismic fragility curves of single storey RC precast structures by comparing different Italian codes", *Earthq. Struct.*, **12**(3), 359-374, <https://doi.org/10.12989/eas.2017.12.3.359>.
- Billah, A.H.M. and Shahria Alam, M. (2014), "Seismic fragility assessment of highway bridges: A state-of-the-art review", *Struct. Infrastruct. Eng.*, **11**(6). <https://doi.org/10.1080/15732479.2014.912243>.
- Building Problem Research Board (1969), *Indonesian Load Regulations 1970*, NI 18.
- Choi, E., DesRoches, R. and Nilesen, B. (2004), "Seismic fragility of typical bridges in moderate seismic zone", *Eng. Struct.*, **26**, 187-199. <https://doi.org/10.1016/j.engstruct.2003.09.006>.
- Crespi, P. *et al.* (2020), "Seismic assessment of six typologies of existing RC bridges", *Infrastruct.*, **5**, 52. <https://doi.org/10.3390/infrastructures5060052>
- Department of Public Works (1992), *Bridge Management System (BMS) 1992*.
- Directorate General of Highways Ministry of Public Works and Housing, Indonesia [<https://data.pu.go.id>]. (26 July 2021).
- Dukes, J., *et al* (2018), "Development of a bridge-specific fragility methodology to improve the seismic resilience of bridges", *Earthq. Struct.*, **15**(3), 253-261, <https://doi.org/10.12989/eas.2018.15.3.253>.
- Federal Emergency Management Agency (2003), *HAZUS-MH MR4 Technical Manual, Multi-Hazard Loss Estimation Methodology: Earthquake Model*. Washington, D.C
- FHWA-NHI (2014), *LRFD Seismic Analysis & Design of Bridges Reference Manual (Publication No. FHWA-NHI-15-004)*. Department of Transportation Federal Highway Administration.
- Han, Q., Dong, H., Du, X. and Zhou, Y. (2015), "Pounding analysis of RC bridge considering spatial variability of ground motions", *Earthq. Struct.*, **9**(5), 1029-1044. <https://doi.org/10.12989/eas.2015.9.5.1029>.
- Hutapea, B.M., Asrurifak, M. and Hendriyawan, H. (2015), Generation of a pair of surface time histories for Jakarta used for earthquake resistance design of infrastructures. *Jurnal Teknologi*.
- Indonesian National Standard (2008), *Bridge Design for Earthquake Loads, SNI 2833:2008*.
- Indonesian National Standard (2016), *Bridge Design for Earthquake Loads, SNI 2833:2016*.
- Karim, K.R. and Yamazaki, F. (2003), "A simplified method of constructing fragility curves for highway bridges", *Earthq. Eng. Struct. D.*, <https://doi.org/10.1002/eqe.291>.
- Kehila, F., Remki, M., Zourgui, N.H. and Kibboua, A. (2021), "Optimal intensity measure of post-tensioned girder highway bridge using fragility curves", *Earthq. Struct.*, **20**(6), 681-696. <https://doi.org/10.12989/eas.2021.20.6.681>.
- Kibboua, A., Naili, M., Benouar, D. and Kehila, F. (2011), "Analytical fragility curves for typical Algerian reinforced concrete bridge piers", *Struct. Eng. Mech.*, **39**(3), 411-425. <https://doi.org/10.12989/sem.2011.39.3.411>.
- Lim, E., Kusumastuti, D., Rildova, Asneindram, M. and Mulyadi, S.S. (2021), "Performance based evaluation of an existing continuous reinforced concrete bridge-a case study", *E3S Web of Conference*, **331**, 0500 8. <https://doi.org/10.1051/e3sconf/202133105008>.
- Maison, B.F. and Speicher, M.S. (2016), "Loading protocols for ASCE 41 backbone curves", *Earthq. Spectra*, **32**(4), 2513-2532. <https://doi.org/10.1193/010816EQS007EP>.
- Mander, J.B. Priestley, M.J.N. and Park, R. (1988), "Theoretical stress-strain model for confined concrete", *J. Struct. Eng.*, **114**, 1804-1824.
- Ministry of Public Works (2002), *Indonesia Earthquake Source and Hazard Map 2002*.
- Ministry of Public Works (2004), *Guidelines for Bridge Design for Earthquake Loads, PdT-04-2004-B*.
- Ministry of Public Works (2010), *Indonesia Earthquake Source and Hazard Map 2010*.
- Ministry of Public Works and Housing (2017), *Indonesia Earthquake Source and Hazard Map 2017*, National Earthquake Study Center.
- Mitchell, *et al* (2010), "Evolution of seismic design provisions in the national building code of Canada", *Can. J. Civil Eng.*, **37**(9), 1157-1170. <https://doi.org/10.1139/L10-054>.

- Moschonas, I.F., Kappos, A.J. and Panetsos, P. (2009), "Seismic fragility curves for Greek bridges: Methodology and case studies", *Bull. Earthq. Eng.*, **7**, 439-468. <https://doi.org/10.1007/s10518-008-9077-2>.
- National Academies of Sciences, Engineering & Medicine (2020), *NCHRP 949 Research Report – Proposed AASHTO Guidelines for Performance-Based Seismic Bridge Design*, Washington D.C.
- Nielson, B.G. and DesRoches, R. (2007), "Analytical seismic fragility curve for typical bridges in the Central and Southern United States", *Earthq. Spectra*, **23**(3), 615-633. <https://doi.org/10.1193/1.2756815>.
- Nielson, B.G. and DesRoches, R. (2007), "Seismic fragility methodology for highway bridges using a component level approach", *Earthq. Eng. Struct. D.*, **36**, 823-839. <https://doi.org/10.1002/eqe.655>.
- Olmos, B.A., Jara, J.M. and Jara, M. (2012), "Influence of some relevant parameters in the seismic vulnerability of RC bridges", *Earthq. Struct.*, **3**(3-4), 365-381.
- Ramanatan, K., DesRoches, R. and Padgett, J.E. (2012), "A comparison of pre-and post-seismic design considerations in moderate seismic zones through the fragility assessment of multispan bridge classes", *Eng. Struct.*, **45**, 559-573. <https://doi.org/10.1016/j.engstruct.2012.07.004>.
- Shekhar, S., Ghosh, J. and Ghosh, S. (2019), "Impact of design code evolution on failure mechanism and seismic fragility of highway bridge piers", *J. Bridge Eng.*, **25**(2), [https://doi.org/10.1061/\(ASCE\)BE.1943-5592.0001518](https://doi.org/10.1061/(ASCE)BE.1943-5592.0001518).
- Shinozuka, M., Saxena, V. and Deodatis, G. (2000), Effect of spatial variation of ground motion on highway structures, Technical Report MCEER-00-0013, December 31, 2000.
- Shinozuka, M., Banerjee, S. and Kim, S.H. (2007), Fragility considerations in highway bridge design, Technical Report MCEER-07-0023, December 14, 2007.
- Simanjuntak, V.C., Imran, I., Moestopo, M. and Setio, H.D. (2022), "The evolution of seismic design provisions in Indonesia's national bridge code", *J. Eng. Tech. Sci.*, <https://doi.org/10.5614/j.eng.technol.sci.2022.54.6.14>.
- Simon, J. and Vigh, L.G. (2016), "Seismic fragility assessment of integral precast multi-span bridges in areas of moderate seismicity", *Bull. Earthq. Eng.*, <https://doi.org/10.1007/s10518-016-9947-y>.
- Simon, J. and Vigh, L.G. (2017), "Parametric seismic evaluation of highway overpass bridges in moderate seismic areas", *Earthq. Struct.*, **12**(3), 375-388. <https://doi.org/10.12989/eas.2017.12.3.375>.
- Stefanidou, S.P. and Kappos, A.J. (2018), "Bridge specific fragility analysis: when is it really necessary?", *Bull. Earthq. Eng.*, <https://doi.org/10.1007/s10518-018-00525-9>.
- SYNER-G (2011), *D2.12–Efficient Intensity Measures for Components Within a Number of Infrastructures*.
- Transportation Research Board of The National Academies (2013), *Performance-Based Seismic Bridge Design NCHRP Synthesis 440*, Washington: TRB.
- TRC/Imbsen (2010), *XTRACT Cross Section Analysis Software for Structural & Earthquake Engineering*.
- Vamvatsikos, D. and Cornell, C.A. (2002), *Incremental Dynamic Analysis, Earthquake Engineering and Structural Dynamic 2002*, **31**, 491-514.
- Waseem, M. and Spacone, E. (2021), "Fragility curves for the typical multi-span simply supported bridges in northern Pakistan", *Struct. Eng. Mech.*, **64**(2), 213-223. <https://doi.org/10.12989/sem.2017.64.2.213>.